Gas-Phase Identity S_N2 Reactions of Halide Anions with Methyl Halides: A High-Level Computational Study

Mikhail N. Glukhovtsev,[1a,b] Addy Pross,*[,1a,c] and Leo Radom*[,1d]

Contribution from the School of Chemistry, University of Sydney, Sydney, NSW 2006, Australia, and Research School of Chemistry, Australian National University, Canberra, ACT 0200, Australia

Received August 5, 1994[⊗]

Abstract: High-level ab initio molecular orbital calculations at the G2(+) level of theory have been carried out for the identity nucleophilic substitution reactions, $X^- + CH_3X \rightarrow XCH_3 + X^-$, where X = F, Cl, Br, and I. The reaction profiles all involve central barriers ($\Delta H^{\ddagger}_{cent}$) which are found to lie within a surprisingly narrow range, decreasing in the order Cl (53.5 kJ mol^{-1}) > F (46.1 kJ mol^{-1}) ≥ Br (45.0 kJ mol^{-1}) > I (40.8 kJ mol^{-1}) at 298 K; the value for X = Cl is in good agreement with a recent experimental determination (55.2 ± 8.4 kJ mol^{-1}). The overall barriers relative to the reactants ($\Delta H^{\ddagger}_{ovr}$) are −11.0 (F), 9.8 (Cl), 4.5 (Br), and 5.5 (I) kJ mol^{-1} at 298 K. Stabilization energies of the ion−molecule complexes (ΔH_{comp}) decrease in the order F (57.1 kJ mol^{-1}) > Cl (43.7 kJ mol^{-1}) > Br (40.5 kJ mol^{-1}) > I (35.3 kJ mol^{-1}) at 298 K and are found to correlate well with halogen electronegativities. A reasonably good correlation between $\Delta H^{\ddagger}_{cent}$ and the ionization energy of X^- is observed. The significance of these results to our understanding of the energetics of gas-phase S_N2 reactions is discussed.

Introduction

Bimolecular nucleophilic substitution (S_N2) at carbon is one of the most important reactions in organic chemistry. In recent years, much effort has been devoted to extending the study of S_N2 reactions to the gas phase, both experimentally[2,3] and theoretically.[2,4−7] Such studies have been particularly valuable as they allow the separation of the various reactivity factors into those that are intrinsic molecular and those that are solvent derived.

Despite the many studies that have been conducted to date, gas-phase barrier heights for the exchange reaction of methyl halides with halide ion (eq 1)

$$X^- + CH_3X \rightarrow XCH_3 + X^- \quad (X = F, Cl, Br, \text{and } I) \quad (1)$$

remain uncertain.[3b,k] Direct experimental data are often difficult to obtain, being close to the limit of current experimental capabilities. Indeed, the values of these barriers have been the subject of continuing debate.[2a,3b,k]

In view of the experimental difficulties, theory would appear to provide an attractive alternative for exploring the S_N2 energy surface, at least for simple systems. Unfortunately, the theoretical approach is not without its own problems. It is clear from the large number of calculations already carried out on reaction 1[4a−e,i−k,q,r,t,u,6−8] that the computational data are very sensitive to the level of theory employed. As has recently been noted by Wladkowski and Brauman,[3k] theory has not yet been able to provide definitive results.

In an attempt to redress this situation, we have examined the set of halide-exchange S_N2 reactions 1 using a level of theory,

⊗ Abstract published in *Advance ACS Abstracts*, January 1, 1995.

(1) (a) University of Sydney. (b) Permanent address: Institute of Physical and Organic Chemistry, Rostov University, 194/3 Stachka Ave., Rostov on Don, 344104, Russian Federation. (c) Permanent address: Ben-Gurion University of the Negev, Beer Sheva, Israel. (d) Australian National University.

(2) Comprehensive collections of both experimental and computational data up to 1991 may be found in the monographs: (a) Shaik, S. S.; Schlegel, H. B.; Wolfe, S. *Theoretical Aspects of Physical Organic Chemistry, The S_N2 Mechanism*; Wiley: New York, 1992. (b) Minkin, V. I.; Simkin, B. Y.; Minyaev, R. M. *Quantum Chemistry of Organic Compounds—Mechanisms of Reactions*; Springer-Verlag: Berlin, 1990.

(3) (a) Van Doren, J. M.; DePuy, C. H.; Bierbaum, V. M. *J. Phys. Chem.* **1989**, *93*, 1130. (b) DePuy, C. H.; Gronert, S.; Mullin, A.; Bierbaum, V. M. *J. Am. Chem. Soc.* **1990**, *112*, 8650. (c) Gronert, S.; DePuy, C. H.; Bierbaum, V. M. *J. Am. Chem. Soc.* **1991**, *113*, 4009. (d) VanOrden, S. L.; Pope, R. M.; Buckner, S. W. *Org. Mass Spectrom.* **1991**, *26*, 1003. (e) Graul, S. T.; Bowers, M. T. *J. Am. Chem. Soc.* **1991**, *113*, 9696. (f) Cyr, D. M.; Posey, L. A.; Bishea, G. A.; Han, C.-C.; Johnson, M. A. *J. Am. Chem. Soc.* **1991**, *113*, 9697. (g) Wladkowski, B. D.; Lim, K. F.; Allen, W. D.; Brauman, J. I. *J. Am. Chem. Soc.* **1992**, *114*, 9136. (h) Cyr, D. M.; Bishea, G. A.; Scarton, M. G.; Johnson, M. A. *J. Chem. Phys.* **1992**, *97*, 5911. (i) Wilbur, J. L.; Wladkowski, B. D.; Brauman, J. I. *J. Am. Chem. Soc.* **1993**, *115*, 10823. (j) Knighton, W. B.; Bognar, J. A.; O'Connor, P. M.; Grimsrud, E. P. *J. Am. Chem. Soc.* **1993**, *115*, 12079. (k) Wladkowski, B. D.; Brauman, J. I. *J. Phys. Chem.* **1993**, *97*, 13158. (l) Giles, K.; Grimsrud, E. P. *J. Phys. Chem.* **1993**, *97*, 1318. (m) Cyr, D. M.; Scarton, G.; Johnson, M. A. *J. Chem. Phys.* **1993**, *99*, 4869. (n) Strode, K. S.; Grimsrud, E. P. *Int. J. Mass Spectrom. Ion Processes* **1994**, *130*, 227. (o) Viggiano, A. A.; Morris, R. A.; Su, T.; Wladkowski, B. D.; Craig, S. L.; Zhong, M.; Brauman, J. I. *J. Am. Chem. Soc.* **1994**, *116*, 2213. (p) Wladkowski, B. D.; Wilbur, J. L.; Brauman, J. I. *J. Am. Chem. Soc.* **1994**, *116*, 2471. (q) Morris, R. A.; Viggiano, A. A. *J. Phys. Chem.* **1994**, *98*, 3740. (r) Graul, S. T.; Bowers, M. T. *J. Am. Chem. Soc.* **1994**, *116*, 3875.

(4) (a) Vande Linde, S. R.; Hase, W. L. *J. Phys. Chem.* **1990**, *94*, 2778. (b) Vande Linde, S. R.; Hase, W. L. *J. Phys. Chem.* **1990**, *94*, 6148. (c) Vande Linde, S. R.; Hase, W. L. *J. Chem. Phys.* **1990**, *93*, 7962. (d) Cho, Y. J.; Vande Linde, S. R.; Zhu, L.; Hase, W. L. *J. Chem. Phys.* **1992**, *96*, 8275. (e) Wolfe, S.; Kim, C.-K. *J. Am. Chem. Soc.* **1991**, *113*, 8056. (f) Zhao, X. G.; Tucker, S. C.; Truhlar, D. G. *J. Am. Chem. Soc.* **1991**, *113*, 826. (g) Kabbaj, O. K.; Lepetit, M. B.; Malrieu, J. P.; Sini, G.; Hiberty, P. C. *J. Am. Chem. Soc.* **1991**, *113*, 5619. (h) Gronert, S. *J. Am. Chem. Soc.* **1991**, *113*, 6041. (i) Shi, Z.; Boyd, R. J. *J. Am. Chem. Soc.* **1991**, *113*, 1072. (j) Jensen, F. *Chem. Phys. Lett.* **1992**, *196*, 368. (k) Sini, G.; Shaik, S.; Hiberty, P. C. *J. Chem. Soc., Perkin Trans. 2* **1992**, 1019. (l) Shi, Z.; Boyd, R. *Can. J. Chem.* **1992**, *70*, 450. (m) Barnes, J. A.; Williams, I. H. *J. Chem. Soc., Chem. Commun.* **1993**, 1286. (n) Gronert, S. *J. Am. Chem. Soc.* **1993**, *115*, 652. (o) Bickelhaupt, F. M.; Baerends, E. J.; Nibbering, N. M. M.; Ziegler, T. *J. Am. Chem. Soc.* **1993**, *115*, 9160. (p) Boyd, R. J.; Kim, C.-K.; Shi, Z.; Weinberg, N.; Wolfe, S. *J. Am. Chem. Soc.* **1993**, *115*, 10147. (q) Shaik, S.; Ioffe, A.; Reddy, A. C.; Pross, A. *J. Am. Chem. Soc.* **1994**, *116*, 262. (r) Hu, W.-P.; Truhlar, D. G. *J. Phys. Chem.* **1994**, *98*, 1049. (s) Poirier, R.; Wang, Y.; Westaway, K. C. *J. Am. Chem. Soc.* **1994**, *116*, 2526. (t) Anh, N. T.; Maurel, F.; Thanh, B. T.; Thao, H. H.; N'Guessan, Y. T. *New J. Chem.* **1994**, *18*, 473. (u) Lee, I.; Kim, C. K.; Chung, D. S.; Lee, B.-S. *J. Org. Chem.* **1994**, *59*, 4490. (v) Hu, W.-P.; Truhlar, D. G. *J. Am. Chem. Soc.* **1994**, *116*, 7797.

(5) Basilevsky, M. V.; Koldobskii, S. G.; Tikhomirov, V. A. *Russ. Chem. Rev. (Engl. Transl.)* **1986**, *55*, 948.

(6) Shi, Z.; Boyd, R. J. *J. Am. Chem. Soc.* **1990**, *112*, 6789.

(7) Vetter, R.; Zülicke, L. *J. Am. Chem. Soc.* **1990**, *112*, 5136.

(8) Dewar, M. J. S.; Healy, E. *Organometallics* **1982**, *1*, 1705.

0002-7863/95/1517-2024$09.00/0

specifically a modification of G2 theory, that is higher than the levels previously employed. At this higher level of theory we hope to obtain more reliable estimates of the energetics of this very basic reaction.

Computational Methods

Standard ab initio molecular orbital calculations[9] were carried out using a modified form of G2 theory[10] with the GAUSSIAN-92 system of programs.[11] G2 theory corresponds effectively to calculations at the QCISD(T)/6-311+G(3df,2p) level with zero-point vibrational energy (ZPE) and higher level corrections. It has been shown[10,12] to perform well for the calculation of atomization energies, ionization energies, electron affinities, bond energies, proton affinities, acidities, and reaction barriers.

Our modifications to G2 theory have been introduced to allow a better description of anions and for computational simplification. In the first place, geometries were optimized and vibrational frequencies determined with a basis set that includes diffuse functions, specifically 6-31+G(d) in place of 6-31G(d) for first- and second-row atoms. In addition, the MP2/6-31+G(d) optimizations were carried out with the frozen-core approximation rather than with all electrons being included in the correlation treatment. Finally, harmonic vibrational frequencies were calculated at the HF/6-31+G(d) level rather than HF/6-31G(d). This level of theory is termed G2(+).

For bromine-containing species, calculations were carried out both with the inclusion of all electrons (AE) and with the use of an effective core potential (ECP) for the core electrons. The all-electron calculations of the Br-containing species were performed at the G2(MP2)(+) level, analogous to G2(MP2).[13] For iodine-containing species, only the ECP procedure, based on the quasirelativistic pseudopotentials developed by Hay and Wadt,[14] was used (G2(+)-ECP). Geometry optimizations were carried out and harmonic frequencies determined using the SV4P basis set, as described previously,[16] for the AE calculations on Br-containing molecules, and with [21/21] valence basis sets[14] supplemented by diffuse functions for the ECP calculations for Br- and I-containing molecules. The diffuse function exponents were found from QCISD(T) calculations on the Br^- and I^- anions with [111/111] valence basis sets, giving values of $\alpha_s(Br) = 0.0640$, $\alpha_p(Br) = 0.0402$, $\alpha_s(I) = 0.0569$, and $\alpha_p(I) = 0.0330$. As noted above, the 6-31+G(d) basis set was used for hydrogen and first- and second-row atoms in geometry and frequency calculations and we refer loosely to such calculations overall (i.e. including Br and I) as MP2/6-31+G(d) or HF/6-31+G(d). The single-point ECP energy calculations for bromine and iodine utilized the uncontracted [111/111] valence basis sets[14] augmented by d and f polarization functions as well as by s and p diffuse functions. The d and f exponents were optimized for HBr and HI at the QCISD(T) level, giving values of $\alpha_d(Br) = 0.427$, $\alpha_f(Br) = 0.574$, $\alpha_d(I) = 0.292$, and $\alpha_f(I) = 0.441$. The splitting factors for the multiple sets of d functions required for the (3df,2p) part of the basis set were taken to be the same as for first- and second-row atoms. The diffuse exponents were given the values noted above. We refer loosely to the ultimate basis set used in our G2(+) calculations as 6-311+G(3df,2p). Full details will be presented elsewhere.[17] Note that we have recommended[17,18] alternative ECP basis sets for bromine and iodine for use in *standard G2-ECP* calculations.

An alternative modified version of G2 theory (G2+), designed particularly for anion calculations, has recently been successfully employed by Gronert[19] in a study of proton-transfer reactions involving anionic species, yielding proton affinities very close to experimental values. In a few test cases, our G2(+) procedure was found to lead to almost the same calculated relative energies as those obtained at the G2+ level (see Table 4 below). We have used G2(+) in the present study because it is computationally less demanding.

In order to obtain energies for the various species involved in reaction 1 at 298 K, vibrational contributions to thermal corrections[9,20] were calculated using the harmonic frequencies computed at HF/6-31+G(d) and scaled by 0.8929.[10]

Charge distributions were obtained from the wave functions calculated at the MP2/6-311+G(3df,2p) level on MP2/6-31+G(d) geometries, employing natural population analysis (NPA).[21] NPA charges in organic molecules have been shown to be satisfactory for the correlation of charges with changes in molecular structure.[22]

Calculated total energies at 0 and 298 K are presented in Table 1. Unless otherwise stated, we have used the results of G2(+)-AE calculations for F- and Cl-containing molecules and G2(+)-ECP calculations for Br- and I-containing molecules in our analysis and have given energy data at 298 K. Throughout this paper, relative energies are presented as enthalpy changes (ΔH) at 0 and/or 298 K, with bond lengths in angstroms and bond angles in degrees.

Results and Discussion

It is now accepted[2-5,24] that the energy profile for reaction 1 may be represented, as proposed by Brauman,[23] by a double-well potential curve (Figure 1). Thus the reaction involves the initial formation of a reactant ion−molecule complex, **1**, with a complexation energy, ΔH_{comp}, relative to separated reactants. This complex must then overcome an activation barrier that we

(9) Hehre, W. J.; Radom, L.; Schleyer, P. v. R.; Pople, J. A. *Ab Initio Molecular Orbital Theory*; Wiley: New York, 1986.

(10) Curtiss, L. A.; Raghavachari, K.; Trucks, G. W.; Pople, J. A. *J. Chem. Phys.* **1991**, *94*, 7221.

(11) Frisch, M. J.; Trucks, G. W.; Head-Gordon, M.; Gill, P. M. W.; Wong, M. W.; Foresman, J. B.; Johnson, B. G.; Schlegel, H. B.; Robb, M. A.; Replogle, E. S.; Gomperts, R.; Andres, J. L.; Raghavachari, K.; Binkley, J. S.; Gonzalez, C.; Martin, R. L.; Fox, D. J.; DeFrees, D. J.; Baker, J.; Stewart, J. J. P.; Pople, J. A. GAUSSIAN-92; Gaussian Inc.: Pittsburgh, PA, 1992.

(12) See, for example: (a) Smith, B. J.; Radom, L. *J. Phys. Chem.* **1991**, *95*, 10549. (b) Ma, N. L.; Smith, B. J.; Pople, J. A.; Radom, L. *J. Am. Chem. Soc.* **1991**, *113*, 7903. (c) Nobes, R. H.; Radom, L. *Chem. Phys. Lett.* **1992**, *189*, 554. (d) Yu, D.; Rauk, A.; Armstrong, D. A. *J. Phys. Chem.* **1992**, *96*, 6031. (e) Wong, M. W.; Radom, L. *J. Am. Chem. Soc.* **1993**, *115*, 1507. (f) Smith, B. J.; Radom, L. *J. Am. Chem. Soc.* **1993**, *115*, 4885. (g) Schlegel, H. B.; Skancke, A. *J. Am. Chem. Soc.* **1993**, *115*, 7465. (h) Goldberg, N.; Hrusák, J.; Iraqi, M.; Schwarz, H. *J. Phys. Chem.* **1993**, *97*, 10687. (i) Armstrong, D. A.; Rauk, A.; Yu, D. *J. Am. Chem. Soc.* **1993**, *115*, 666. (j) Wiberg, K.; Rablen, P. R. *J. Am. Chem. Soc.* **1993**, *115*, 9234. (k) Wiberg, K.; Nakaji, D. *J. Am. Chem. Soc.* **1993**, *115*, 10658. (l) Lammertsma, K.; Prasad, B. V. *J. Am. Chem. Soc.* **1994**, *116*, 642. (m) Gauld, J. W.; Radom, L. *J. Phys. Chem.* **1994**, *98*, 777. (n) Chiu, S.-W.; Li, W.-K.; Tzeng, W-B.; Ng, C.-Y. *J. Chem. Phys.* **1992**, *97*, 6557. (o) Durant, J. L.; Rohlfing, C. M. *J. Chem. Phys.* **1993**, *98*, 8031. (p) Glukhovtsev, M. N.; Pross, A.; Radom, L. *J. Am. Chem. Soc.* **1994**, *116*, 5961.

(13) Curtiss, L. A.; Raghavachari, K.; Pople, J. A. *J. Chem. Phys.* **1993**, *98*, 1293.

(14) Wadt, W. R.; Hay, P. J. *J. Chem. Phys.* **1985**, *82*, 284. These pseudopotentials have recently been successfully employed in calculations on CH_3X (X = F, Br, Cl, I),[15a,b] on the gas-phase complexes of hydrohalogens,[15c] and on the $I^-\cdots CH_3I$ complex.[4r]

(15) (a) Schneider, W.; Thiel, W. *J. Chem. Phys.* **1987**, *86*, 923. (b) Schneider, W.; Thiel, W. *Chem. Phys.* **1992**, *159*, 49. (c) Müller, B.; Reinhold, J. *Chem. Phys. Lett.* **1992**, *196*, 363.

(16) McGrath, M. P.; Radom, L. *J. Chem. Phys.* **1991**, *94*, 511.

(17) Glukhovtsev, M. N.; Pross, A.; McGrath, M. P.; Radom, L. *J. Chem. Phys.*, submitted for publication.

(18) Gluthovtsev, M. N.; Szulejko, J. E.; McMahon, T. B.; Gauld, J. W.; Scott, A. P.; Smith, B. J; Pross, A.; Radom, L. *J. Phys. Chem.* **1994**, *98*, 13099.

(19) Gronert, S. *J. Am. Chem. Soc.* **1993**, *115*, 10258.

(20) Daudel, R.; Leroy, G.; Peeters, D.; Sana, M. *Quantum Chemistry*; Wiley: New York, 1983.

(21) (a) Reed, A. R.; Weinstock, R. B.; Weinhold, F. *J. Chem. Phys.* **1985**, *83*, 735. (b) Reed, A. E.; Curtiss, L. A.; Weinhold, F. *Chem. Rev.* **1988**, *88*, 899. (c) Weinhold, F.; Carpenter, J. E. In *The Structure of Small Molecules and Ions*; Naaman, R., Vager, Z., Eds.; Plenum Press: New York, 1988; p 227. (d) Reed, A. E.; Weinhold, F. *Isr. J. Chem.* **1991**, *31*, 277. For recent NPA applications, see, e.g.: (e) Reed, A. E.; Schleyer, P. v. R. *J. Am. Chem. Soc.* **1990**, *112*, 1434. (f) Glukhovtsev, M. N.; Schleyer, P. v. R. *Chem. Phys. Lett.* **1992**, *198*, 547. (g) Mestres, J.; Duran, M.; Bertran, J. *Theor. Chim. Acta* **1994**, *88*, 325.

(22) Wiberg, K. B.; Rablen, P. R. *J. Comput. Chem.* **1993**, *14*, 1504.

(23) (a) Olmstead, W. N.; Brauman, J. I. *J. Am. Chem. Soc.* **1977**, *99*, 4219. (b) Pellerite, M. J.; Brauman, J. I. *J. Am. Chem. Soc.* **1980**, *102*, 5993. (c) Pellerite, M. J.; Brauman, J. I. *J. Am. Chem. Soc.* **1983**, *105*, 2672. (d) Pellerite, M. J.; Brauman, J. I. In *Mechanistic Aspects of Inorganic Reactions*; Rorabacher, D. R., Endicott, J. F., Eds.; ACS Symp. Ser.; American Chemical Society: Washington, DC, 1982; Vol. 198, p 81.

(24) Riveros, J. M.; Jose, S. M.; Takashima, K. *Adv. Phys. Org. Chem.* **1985**, *21*, 197.

Table 1. Calculated G2(+) Total Energies (hartrees) for Species Involved in the Identity Reaction of X^- with CH_3X[a]

species	0 K	298 K
F^-	−99.760 69[b]	−99.758 33
CH_3F	−139.554 12[b]	−139.550 25
$F^-\cdots CH_3F$ (**1a**)	−239.336 33[b]	−239.330 33
FCH_3F^- (**2a**)	−239.317 86[b]	−239.312 79
Cl^-	−459.808 99	−459.806 63
CH_3Cl	−499.553 85	−499.549 87
$Cl^-\cdots CH_3Cl$ (**1b**)	−959.379 58	−959.373 13
$ClCh_3Cl^-$ (**2b**)	−959.358 45	−959.352 75
Br^-	−13.229 29[c,d]	−13.226 93
CH_3Br	−52.961 93[c,d]	−52.957 86
$Br^-\cdots CH_3Br$ (**1c**)	−66.206 86[c,d]	−66.200 22
$BrCH_3Br^-$ (**2c**)	−66.189 02[c,d]	−66.183 07
I^-	−11.446 98	−11.444 62
CH_3I	−51.172 82	−51.168 68
$I^-\cdots CH_3I$ (**1d**)	−62.633 52	−62.626 73
ICH_3I^- (**2d**)	−62.617 31	−62.611 20

[a] Values listed are all-electron (AE) G2(+) energies for F- and Cl-containing species and effective-core-potential (ECP) G2(+) energies for Br- and I-containing species. [b] G2+ energies are −99.755 91 (F^-), −139.553 64 (CH_3F), −239.332 08 ($F^-\cdots CH_3F$, **1a**) and −239.312 34 (FCH_3F^-, **2a**) hartrees. [c] G2(+)(MP2)−AE energies are −2 572.648 49 (Br^-), −2 612.381 34 (CH_3Br), −5 185.043 17 ($Br^-\cdots CH_3Br$, **1c**), and −5 185.025 07 ($BrCH_3Br^-$, **2c**) hartrees. [d] G2(+)(MP2)−ECP energies are −13.218 47 (Br^-), −52.952 40 (CH_3Br), −66.186 48 ($Br^-\cdots CH_3Br$, **1c**), and −66.168 02 ($BrCH_3Br^-$, **2c**) hartrees.

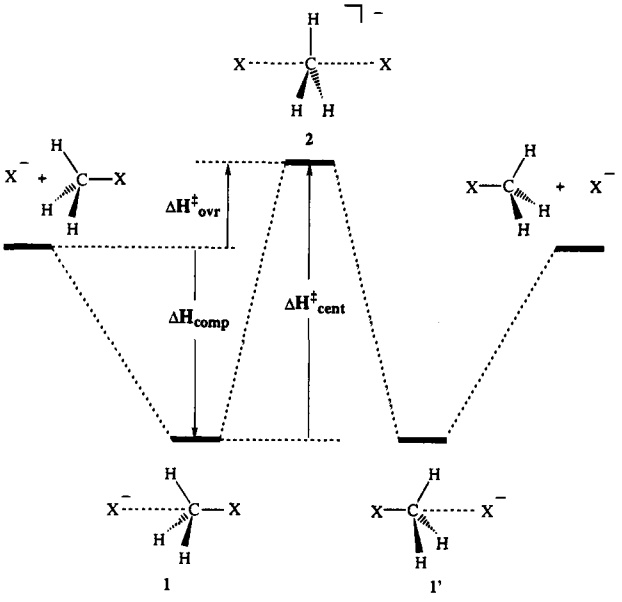

Figure 1. Schematic energy profile for the X^- + CH_3X identity exchange reaction (X = F to I).

term the *central* barrier, $\Delta H^{\ddagger}_{cent}$, to reach the transition structure, **2**, which then breaks down into the product ion−molecule complex, **1′**. Finally, the product ion−molecule complex dissociates into separated products. The *overall* activation barrier relative to separated reactants (rather than to the complex) is denoted $\Delta H^{\ddagger}_{ovr}$. For the set of identity reactions described here, reactants and products are of course identical, as are the reactant ion−molecule and product ion−molecule complexes.

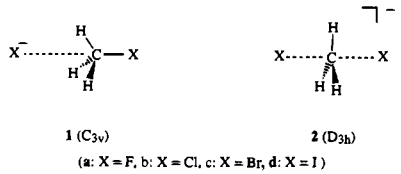

Table 2. Calculated and Experimental Geometries of CH_3X (X = F, Cl, Br, and I)

species	level[a]	r(C−X)	r(C−H)	∠XCH
CH_3F	MP2/6-31G(d)	1.392[b]	1.092[b]	109.1[b]
	MP2/6-31+G(d)	1.407	1.090	108.0
	MP2/6-31++G(d,p)[c]	1.405	1.087	108.2
	expt[d]	1.383	1.086	108.8
CH_3Cl	MP2/6-31G(d)	1.779[b]	1.088[b]	108.9[b]
	MP2/6-31+G(d)	1.780	1.089	108.9
	expt[e]	1.776	1.085	108.6
CH_3Br	MP2/6-31G(d)−AE	1.951[f]	1.087[f]	107.8[f]
	MP2/6-31+G(d)−AE	1.949	1.088	107.9
	MP2/6-31+G(d)−ECP	1.954	1.088	108.0
	expt[g]	1.934	1.082	107.7
CH_3I	MP2/6-31+G(d)−ECP	2.140	1.088	108.0
	expt[h]	2.132	1.085	108.6

[a] Bond lengths in Å. See text for details of the Br and I basis sets. [b] From ref 12 m. Frozen-core approximation used. [c] Level used for G2+ theory.[19] [d] From ref 25. [e] From ref 26. [f] Frozen-core approximation used. [g] From ref 27. [h] From ref 28.

Table 3. NPA charge Distributions for CH_3X (X = F, Cl, Br, and I)[a]

species		q(X)	q(C)	q(H)
CH_3F		−0.400	0.050	0.150
CH_3Cl		−0.063	−0.531	0.198
CH_3Br	AE	−0.004	−0.614	0.206
	ECP	0.016	−0.638	0.207
CH_3I	ECP	0.121	−0.757	0.212

[a] Calculated at the MP2/6-311+G(3df,2p) level. See text for details of the Br and I basis sets.

A. CH_3X Structures (X = F, Cl, Br, and I). Calculated CH_3X geometries are shown in Table 2 and are in reasonable agreement with experiment.[25-27] The theoretical C−X bond lengths differ from the experimental values by up to 0.024 Å (for CH_3F) while the largest deviation for the C−H bond lengths is 0.006 Å (for CH_3Br). The calculated ∠XCH angles differ from experimental values by up to 0.6°. We note that MP2 calculations with larger basis sets (e.g. 6-311+G(2df,p)) give quite precise agreement with experimental geometries for CH_3X systems.[12m]

Calculated charge distributions in the CH_3X molecules are presented in Table 3. These data show that the fluorine atom in CH_3F bears considerable negative charge, in contrast to the situation for the other CH_3X molecules where chlorine and bromine have almost zero charge while iodine actually has a positive charge.

B. Ion−Molecule Complexes. There are various conceivable geometries for these complexes. For example, the halide ion can coordinate with the carbon and three hydrogens (**1**), with two hydrogens (**3**), with just one hydrogen (**4**), or with the halogen atom of the CH_3X molecule (**5**).

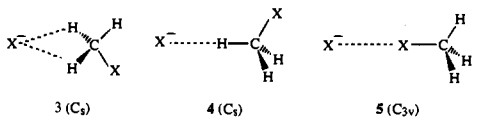

(25) Egawa, T.; Yamamoto, S.; Nakata, M.; Kuchitsu, K. *J. Mol. Struct.* **1987**, *156*, 213.
(26) Jensen, T.; Brodersen, S.; Guelachvili, G. *J. Mol. Spectrosc.* **1981**, *88*, 378.
(27) Graner, G. *J. Mol. Spectrosc.* **1981**, *90*, 394.
(28) Harmony, M. D.; Laurie, V. W.; Kuczkowski, R. L.; Ramsay, D. A.; Lovas, F. J.; Lafferty, W. J.; Maki, A. G. *J. Phys. Chem. Ref. Data* **1979**, *8*, 619.

Table 4. Complexation Energies (ΔH_{comp}) of the Ion−Molecule Complexes, Overall Barrier Heights Relative to Reactants ($\Delta H^{\ddagger}_{ovr}$), and Central Barriers ($\Delta H^{\ddagger}_{cent}$) of Reaction 1, Calculated with Various Modifications of G2 Theory (kJ mol^{-1})[a]

X	level	ΔH_{comp}	$\Delta H^{\ddagger}_{ovr}$	$\Delta H^{\ddagger}_{cent}$
F	G2(+)	56.5 (57.1)	−8.0 (−11.0)	48.5 (46.1)
	G2+	59.1	−7.3	51.8
Cl	G2(MP2)(+)	44.3	10.3	54.6
	G2(+)	44.0 (43.7)	11.5 (9.8)	55.5 (53.5)
	Exptl	51.0 ± 8.4[b]	4.2 ± 4.2[c]	55.2 ± 8.4[c]
		36.0 ± 0.8[d]	10.5[e]	
Br	G2(MP2)(+)−AE	35.0	12.5	47.5
	G2(MP2)(+)−ECP	41.0	7.5	48.5
	G2(+)−ECP	41.1 (40.5)	5.8 (4.5)	46.9 (45.0)
	Exptl	38.5 ± 2.1[d]	5.4[f]	46.9[g]
I	G2(+)−ECP	36.0 (35.3)	6.5 (5.5)	42.5 (40.8)
	Exptl	37.7 ± 0.8[d]		
		36.7 ± 1.9[h,i]		

[a] Calculated energies at 0 K are listed, with 298 K values given in parentheses. [b] From ref 34. [c] From ref 33. [d] From ref 35. [e] From ref 3k. The overall barrier determined from modeling the bimolecular kinetics with statistical phase space theory is 11.6 ± 1.0 kJ mol^{-1} at 0 K, see ref 3r. [f] From ref 3i. [g] From ref 23b,c. [h] From ref 3m. [i] A correction for the binding energy of neutral I···CH$_3$I at the I$^-$···CH$_3$I geometry leads to a complexation energy of 33.1 kJ mol^{-1}: see ref 4r.

Previous studies[29−31] suggest **3** and **4** to be higher in energy than **1**. Complex **5** might correspond to the intermediate for the so-called X-philic reaction which results in nucleophilic attack at halogen.[32] Such a mechanism has been suggested[33] for the chloride exchange in the $CH_3Cl + Cl^-$ system at energies higher than 0.5 eV. For X = I, our calculations indicate that while **5** is a minimum, it is 16.6 kJ mol^{-1} higher in energy than **1** at the G2(+) level, consistent with the computational results of Hu and Truhlar.[4r] Since the positive charge on I in CH_3I (Table 3) is most likely to contribute to some stabilization of complex **5** compared with **1**, it would seem likely that for the other halogens (which bear a negative charge on X) **5** is also higher in energy than **1**. Accordingly, complex **1** is presumed to be the most stable structure for the intermediate ion−molecule complex for all four halogens, and we have only examined this structure in the present work.

1. Complexation Energies. G2(+) complexation energies (ΔH_{comp}, see Figure 1) are compared with available experimental data in Table 4. Our theoretical results are in satisfactory agreement with experiment. For example, the calculated complexation energy of Cl$^-$···CH$_3$Cl at 298 K (43.7 kJ mol^{-1}) lies between the most recent experimental value[34] of 51.0 ± 8.4 kJ mol^{-1} and an earlier HPMS value[35] of 36.0 ± 0.8 kJ mol^{-1}. The G2(+) complexation energy of Br$^-$···CH$_3$Br (40.5 kJ mol^{-1} at 298 K) is in good agreement with the HPMS experimental value[35a] of 38.5 ± 2.1 kJ mol^{-1}. The G2(MP2)-(+)−AE value is 34.5 kJ mol^{-1}. Finally, the G2(+) complexation energy of I$^-$···CH$_3$I (35.3 kJ mol^{-1} at 298 K) is close to the experimental HPMS value[35a] of 37.7 ± 0.8 kJ mol^{-1}, as well as the value[3m] derived from the photoelectron spectrum (36.7 ± 1.9 kJ mol^{-1} at 0 K). However, whereas the early HPMS experiments indicated that the complexation energies for **1** with X = Cl, Br, and I are scattered within a narrow range of just 2.5 kJ mol^{-1}, our calculations predict a monotonic decrease through this sequence totalling 8.4 kJ mol^{-1}.

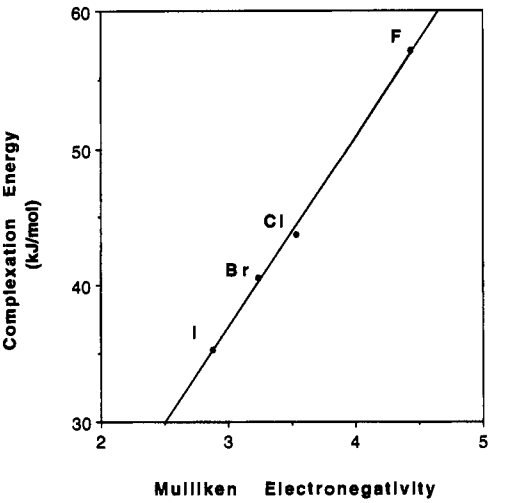

Figure 2. Plot of the G2(+) complexation energies (ΔH_{comp}, 298 K) of the ion−molecule complexes (**1**) vs Mulliken electronegativities (in Pauling units, taken from ref 36b) of the halogen atom.

Table 5. NPA Charge Distributions for the X···CH$_3$X Ion−Molecule Complexes (**1**, X = F, Cl, Br, and I)[a]

species		$q(X_a)$[b]	$q(X_b)$[b]	q(C)	q(H)
1a (X = F)		−0.973	−0.467	−0.052	0.164
1b (X = Cl)		−0.981	−0.150	−0.505	0.212
1c (X = Br)	AE	−0.973	−0.112	−0.565	0.217
	ECP	−0.974	−0.088	−0.595	0.219
1d (X = I)	ECP	−0.973	0.009	−0.708	0.224

[a] Calculated at the MP2/6-311+G(3df,2p) level. See text for details of the Br and I basis sets. [b] $q(X_a)$ is the charge on the incoming halide anion while $q(X_b)$ is the charge on the halogen atom in the CH$_3$X moiety.

In general, our calculated complexation energies are close to results obtained from previous high-level calculations. Thus, CISD/DZDP calculations of Vetter and Zülicke[7] gave 54.8 (X = F), 36.8 (X = Cl), and 35.1 (X = Br) kJ mol^{-1} while MP2/TZ3P+R+(2f,d) calculations of Allen, Brauman, et al.[3g] led to an extrapolated MP∞ value of 44.4 kJ mol^{-1} for X = Cl. Hu and Truhlar[4r] find a large basis set counterpoise-corrected MP2 value of 32.2 kJ mol^{-1} for X = I. We estimated the basis set superposition error (BSSE) in our calculations by computing counterpoise corrections to the G2(+) complexation energy of **1** with X = Cl. The calculated BSSE is found to be just 3.8 kJ mol^{-1}.

For X = Cl, Br, and I, the complexation energies at 298 K are slightly smaller than those at 0 K. However, the complexation energy of F$^-$···CH$_3$F is 0.6 kJ mol^{-1} greater at 298 K than at 0 K (Table 4).

Our G2(+) complexation energies for X$^-$···CH$_3$X (X = F, Cl, Br, and I) are found to decrease in the order F > Cl > Br > I and show a very good linear correlation with electronegativity using the Mulliken (R^2 = 0.998), Pauling (R^2 = 1.000), or Allred-Rochow (R^2 = 0.991) electronegativity scales for halogen.[36] The correlation with the Mulliken scale is shown in Figure 2. The calculated charges (Table 5) suggest that charge transfer in the X$^-$···CH$_3$X complexes is very small and

(29) Schlegel, H. B.; Mislow, K.; Bernardi, F.; Bottoni, A. *Theor. Chim. Acta* **1977**, *44*, 245.
(30) Mitchell, D. J. Ph.D. Thesis, Queen's University, Kingston, Canada, 1981.
(31) Cremer, D.; Kraka, E. *J. Phys. Chem.* **1986**, *90*, 33.
(32) Zefirov, N. S.; Makhon'kov, D. I. *Chem. Rev.* **1982**, *82*, 615.
(33) Barlow, S. E.; Van Doren, J. M.; Bierbaum, V. M. *J. Am. Chem. Soc.* **1988**, *110*, 7240.
(34) (a) Larson, J. W.; McMahon, T. B. *J. Am. Chem. Soc.* **1984**, *106*, 517. (b) Larson, J. W.; McMahon, T. B. *J. Am. Chem. Soc.* **1985**, *107*, 766.
(35) (a) Dougherty, R. C.; Roberts, J. D. *Org. Mass Spectrom.* **1974**, *8*, 81. (b) Dougherty, R. C.; Dalton, J.; Roberts, J. D. *Org. Mass Spectrom.* **1974**, *8*, 77.
(36) For a discussion of the current status of the electronegativity concept in chemistry and for leading references, see: (a) Allen, L. C. *Int. J. Quantum Chem.* **1994**, *49*, 253. (b) Allen, L. C. *J. Am. Chem. Soc.* **1989**, *111*, 9003. (c) Bratsch, S. G. *J. Chem. Educ.* **1988**, *65*, 34. (d) Meek, T. L. *J. Chem. Educ.* **1993**, *70*, 799.

Table 6. Geometries of Ion–Molecule Complexes $X^-\cdots CH_3X$ (**1**, X = F, Cl, Br, and I)

species	level[a]	r(X···C)[b]	r(C–X)[b]	r(C–H)	∠HCX[b]
1a (X = F)	MP2/6-31+G(d)	2.628	1.456	1.084	107.7
	MP2/6-31++G(d,p)	2.609	1.453	1.080	107.8
1b (X = Cl)	MP2/6-31+G(d)	3.270	1.810	1.085	108.8
1c (X = Br)	MP2/6-31+G(d)–AE	3.359	1.983	1.084	107.6
	MP2/6-31+G(d)–ECP	3.395	1.988	1.084	107.8
1d (X = I)	MP2/6-31+G(d)–ECP	3.639	2.170	1.085	107.7

[a] Bond lengths in Å. See text for details of the Br and I basis sets. [b] r(X···C) is the distance between the carbon and incoming halide anion while r(C–X) and ∠HCX$_b$ are the C–X$_b$ bond length and the ∠HCX$_b$ valence angle, respectively, in the CH_3X moiety.

that the binding of X^- to CH_3X is therefore primarily electrostatic (charge-dipole) in character.[3g,34]

2. Geometries. Calculated geometries of complexes **1a–d** are presented in Table 6. The geometries of the CH_3X moieties in the $X^-\cdots CH_3X$ complexes differ only slightly from those in the unperturbed CH_3X molecules (Table 2). The MP2(fc)/6-31+G(d) geometries for X = F and Cl are close to those found at the MP2(full)/6-31+G(d) level.[4e,6]

Comparing theoretical and experimental assessments of the effect of complexation on geometry is of interest. According to a Franck–Condon analysis of the photoelectron spectrum of $I^-\cdots CH_3I$ (**1d**),[3m] the elongation of the C–I bond length in the complex is 0.068 ± 0.005 Å, and the change in the length of the C–H bond (presumed to be a shortening[3m]) within the $I^-\cdots CH_3I$ complex is 0.020 ± 0.005 Å. The ∠ICH angle is estimated to decrease by 1.9°. Our calculations indicate an elongation of the C–I bond by 0.028 Å, a shortening of the C–H bond by 0.002 Å, and a decrease in the ∠ICH angle of 0.3° (Tables 2 and 6). Our MP2 calculated values are in reasonable agreement with the results of recent higher level calculations,[4r] including all-electron MP2 calculations using an augmented polarized triple-ζ quality basis set and QCISD(T) calculations with an augmented polarized double-ζ quality basis set that show changes of +0.026 (MP2) and +0.040 Å (QCISD(T)) for the C–I bond length, −0.003 Å (both MP2 and QCISD(T)) for the C–H bond length, and +0.33° and −0.16° for the ∠ICH angle. An increase in the C–X length, a slight shortening of the C–H length, and a slight decrease in the ∠XCH angle are characteristic features of our results for the other complexes (**1a–c**) as well. The largest percentage C–X bond elongation associated with complex formation is for X = F (3.5%). This is consistent with $F^-\cdots CH_3F$ exhibiting the largest complexation energy (Table 4). The corresponding bond elongation for X = Cl and Br are only 1.7%. The $I^-\cdots CH_3I$ complex which has the lowest complexation energy also exhibits the smallest C–X bond elongation (just 1.4%). We note that the changes in geometry on complexation calculated at the AE and ECP levels for X = Br are very similar.

C. Transition Structures and Barrier Heights. We consider only transition structure **2**, obtained from back-side attack in reaction 1, since front-side attack, involving the formation of a transition structure with four-electron three-center cyclic delocalization,[5] has been found to be associated with much higher barriers.[2b,5,29,37] G2(+) values for the central barriers ($\Delta H^{\ddagger}_{cent}$) and the overall barriers relative to separated reactants ($\Delta H^{\ddagger}_{ovr}$) are included in Table 4. The geometries and charge distributions of the D_{3h} transition structures (**2**) are presented in Tables 7 and 8, respectively.

1. Barriers. Calculated central barriers ($\Delta H^{\ddagger}_{cent}$) are found to be surprisingly similar for the entire set of systems with X = F, Cl, Br, and I, ranging (at 298 K) from 40.8 kJ mol^{-1} for I up to 53.5 kJ mol^{-1} for Cl. Interestingly, the barrier ordering (Cl > F ≥ Br > I) does not follow periodic table ordering. Given the large differences in the bonding characteristics of the halogens (e.g., the C–X bond strengths in CH_3X vary[38] from about 230 to 465 kJ mol^{-1}, see Table 11 below), the small reactivity range might appear surprising. We are inclined to attribute the similarity in the barriers to the fact that the S_N2 transition state involves both the making *and* the breaking of a bond to X (though this is not to say that *all* identity exchange reactions would exhibit similar barriers; for X = H, for example, the barrier is much higher). Thus, factors that would *stabilize* the transition state[39] from the point of view of the nucleophile (e.g., strong nucleophile–carbon bond) will *destabilize* the transition state from the point of view of the leaving group. If there is such an interplay of effects, it is likely to make a simple rationalization of the small differences in calculated barriers more difficult.

Table 7. Geometries of the XCH_3X^- Transition Structures (**2**, X = F, Cl, Br, and I)[a]

species	level	r(X···C)	r(C–H)	% C–X‡ [b]
2a (X = F)	MP2/6-31+G(d)	1.837	1.074	26.2
	MP2/6-31++G(d,p)	1.832	1.071	26.1
2b (X = Cl)	MP2/6-31+G(d)	2.317	1.073	28.0
2c (X = Br)	MP2/6-31+G(d)–AE	2.466	1.074	24.4
	MP2/6-31+G(d)–ECP	2.480	1.074	24.7
2d (X = I)	MP2/6-31+G(d)–ECP	2.673	1.075	23.2

[a] Bond lengths in Å. See text for details of the Br and I basis sets. [b] % C–X‡ is the MP2-calculated index of bond cleavage in transition structures **2** (see eq 2).

Table 8. NPA Charge Distributions for the XCH_3X^- Transition Structures (**2**, X = F, Cl, Br, and I)[a]

species		q(X)	q(C)	q(H)	q(CH$_3$)[b]
2a (X = F)		−0.716	−0.042	0.158	0.432
2b (X = Cl)		−0.628	−0.345	0.200	0.254
2c (X = Br)	AE	−0.597	−0.420	0.205	0.195
	ECP	−0.594	−0.430	0.206	0.188
2d (X = I)	ECP	−0.549	−0.529	0.209	0.098

[a] Calculated at the MP2/6-31+G(3df,2p) level. [b] The CH_3 group charge provides an estimate of the extent of the contribution of the VB triple-ion $X^-R^+X^-$ configuration, see text.

It would be of interest to compare our theoretical results with experimental data. Unfortunately, there is only a limited amount of direct experimental data available for the barriers to reaction 1. If the barrier for an ion–molecule reaction is higher than ca. 9–10 kJ mol^{-1} relative to reactants, the reaction is too slow to be studied at room temperature using ICR spectrometry.[3a,c,k] Accordingly, thermoneutral identity S_N2 reactions which have no thermodynamic driving force to lower the barrier height are generally very slow in the gas phase, and experimental data have only been obtained for reaction 1 when X = Cl. Measurement of the rate coefficients of this reaction at temperatures above 300 K and analysis using a simplified modification of RRKM theory has led[33] to a $\Delta H^{\ddagger}_{cent}$ value of 55.2 ± 8.4 kJ mol^{-1}, in good agreement with our G2(+) result of 53.5 kJ mol^{-1} at 298 K.

Our G2(+) $\Delta H^{\ddagger}_{ovr}$ value (at 298 K) for X = Cl is 9.8 kJ mol^{-1}. While Bierbaum et al.[33] reported 4.2 ± 4.2 kJ mol^{-1} (quoted as 1 ± 1 kcal mol^{-1}) for this barrier, a more recent experimental estimate from Brauman's laboratory[3k] is 10.5 kJ mol^{-1}. From a theoretical analysis based on semiclassical variational transition-state theory, Truhlar[40] found that a $\Delta H^{\ddagger}_{ovr}$ value of 13.0 kJ mol^{-1} reproduces the experimental[33] rate

(37) Anh, N. T.; Minot, C. *J. Am. Chem. Soc.* **1980**, *102*, 103.

(38) Lias, S. G.; Bartmess, J. E.; Liebman, J. F.; Holmes, J. L.; Levin, R. D.; Mallard, W. G. *J. Phys. Chem. Ref. Data* **1988**, *17*, Suppl. 1.

(39) Bach, R. D.; Wolber, G. J. *J. Am. Chem. Soc.* **1984**, *106*, 1401.

coefficient at 300 K. Our theoretical measure agrees quite well with these last two results.[41] Also, our G2(+) $\Delta H^{\ddagger}_{ovr}$ value (at 0 K) for X = Cl (11.5 kJ mol^{-1}) is in good agreement with the barrier determined from modeling the bimolecular kinetics with statistical phase space theory (11.6 ± 1.0 kJ mol^{-1} at 0 K).[3r]

We have calculated the various G2(MP2)(+) energy quantities associated with reaction 1 for X = Br using both all-electron (AE) and effective-core-potential (ECP) calculations. As can be seen from Table 4, the results of G2(MP2)(+)-AE and G2(MP2)(+)-ECP calculations are reasonably close to one another. The $\Delta H^{\ddagger}_{cent}$ values differ by 1 kJ mol^{-1} while the $\Delta H^{\ddagger}_{ovr}$ and ΔH_{comp} values differ by 5−6 kJ mol^{-1}. This provides a measure of confidence in the use of the G2(+)−ECP scheme for calculations of reaction 1 with X = Br as well as for X = I. Unless otherwise noted, we have used the G2(+)-ECP results as the basis for our analysis. However, it is not entirely clear that the G2(+)-ECP results are necessarily better than the G2(MP2)(+)-AE values.

Direct experimental data for the activation barrier, $\Delta H^{\ddagger}_{cent}$, for reaction 1 when X = Br and I are not available. However, our G2(+) value of 45.0 kJ mol^{-1} (Table 4) for X = Br is in good agreement with an indirect experimental estimate by Brauman[23b−d] of 46.9 kJ mol^{-1} and is also close to the results of CISD calculations (45.6 kJ mol^{-1}).[7]

Our $\Delta H^{\ddagger}_{ovr}$ value of 4.5 kJ mol^{-1} for X = Br is in good agreement with Brauman's experimental result of 5.4 kJ mol^{-1} (estimated from the $Cl^- + CH_3Cl$ and $Cl^- + CH_3Br$ reactions).[3k] On the basis of an indirect estimate of the efficiency of the $Br^- + CH_3Br$ reaction, DePuy, Bierbaum, et al.[3b] have concluded that the efficiencies of reaction 1 with X = Cl and Br are similar, suggesting similar $\Delta H^{\ddagger}_{ovr}$ values. Our preferred calculated $\Delta H^{\ddagger}_{ovr}$ values for X = Cl (9.8 kJ mol^{-1}) and Br (G2(+)-ECP) (4.5 kJ mol^{-1}) suggest a difference of ca. 5 kJ mol^{-1}. We note, however, that at the G2(+)(MP2)-AE level, the predicted $\Delta H^{\ddagger}_{ovr}$ values at 298 K are 8.6 (X = Cl) and 11.2 (X = Br) kJ mol^{-1}.

The value of $\Delta H^{\ddagger}_{cent}$ for reaction 1 with X = F has been the subject of some debate. By using kinetic and thermodynamic data for reaction 1 with X = Cl and for the cross-reaction of F^- with CH_3Cl, the $\Delta H^{\ddagger}_{cent}$ value for X = F was estimated by Brauman et al.[23] to be 109.6 kJ mol^{-1}. However, on the basis of the $HO^- + CH_3F$ and $CH_3O^- + CH_3F$ cross-reactions, the barrier for the $F^- + CH_3F$ reaction was concluded by DePuy, Bierbaum, et al.[3b] to be similar to that (55.2 kJ mol^{-1})[33] for the $Cl^- + CH_3Cl$ reaction. The reason for the different experimental estimates remains unresolved at present.[3k] Our G2(+) values of $\Delta H^{\ddagger}_{cent}$ for X = F (46.1 kJ mol^{-1}) and Cl (53.5 kJ mol^{-1}) (Table 3) appear to support the view[3b] that these two barriers are similar in magnitude.

The G2(+) $\Delta H^{\ddagger}_{ovr}$ value for reaction 1 with X = F is *negative* (−11.0 kJ mol^{-1} at 298 K) compared with *positive* values found for the other halogens. This constrasts with CISD results[7] but is in agreement with both MP2/6-31+G(d) calculations[4e,6] and VB calculations.[4k] The $\Delta H^{\ddagger}_{ovr}$ value is found to be 20.8 kJ mol^{-1} lower for X = F than for X = Cl. A lower $\Delta H^{\ddagger}_{ovr}$ value for X = F than that for X = Cl was first pointed out by Keil and Ahlrichs[42] although their CEPA values were all too high. Our result is in qualitative agreement with predictions based on empirical correlations.[43] A possible explanation for the lower relative energy of the FCH_3F^- transition structure compared with the other transition structures may lie in the large contribution of the triple-ion VB configuration, $F^-CH_3^+F^-$ (see below).

Our G2(+) data for $\Delta H^{\ddagger}_{ovr}$ do not support the view expressed recently that, for systems with higher-row halogens (X = Cl, Br), the correlation energy contribution to the barrier height is positive, i.e., the magnitude of the correlation energy is smaller in the transition region than in the reactants.[7] We find that, for X = Cl, Br, and I, higher-level treatments of electron correlation lead to stabilization of the transition structures relative to the reactants compared with both the HF and MP2 data.

Thermal corrections to 298 K lead to small lowerings of both the central barriers ($\Delta H^{\ddagger}_{cent}$) and the overall barriers ($\Delta H^{\ddagger}_{ovr}$) (Table 4).

2. Geometries. The C−H bond lengths in structures **2a−d** are similar (Table 7). This confirms an earlier computational finding by Wolfe[4e] that these bond lengths do not depend strongly on X. The looseness (% $C-X^{\ddagger}$) of transition structure **2** has been defined as:

$$\% \; C-X^{\ddagger} = 100(d^{\ddagger}_{C-X} - d^{comp}_{C-X})/d^{comp}_{C-X} \qquad (2)$$

where $d^{\ddagger}_{C-X}$ and d^{comp}_{C-X} are the C−X bond lengths in transition structure **2** and ion−molecule complex **1**, respectively.[2a,4e] We find that % $C-X^{\ddagger}$ decreases in the order Cl > F > Br > I (Table 7).

3. Charge Distributions. Charge distributions in **2** (Table 8) suggest a contribution of the triple-ion valence bond (VB) configuration, $X^-R^+X^-$, for all halogens, but it is particularly pronounced for X = F. This is in agreement with the recent discussion by Shaik et al.[4k] that emphasized the importance of the triple-ion configuration in the reaction $F^- + CH_3F$. The NPA halogen charges are found to be in reasonable agreement with Bader charges (AIM).[4i] For example, at the MP2 level, the NPA charge on F is −0.716 while the AIM charge is −0.762.[4i] It is reassuring that the AE and ECP charge distributions for X = Br are similar, thereby increasing our confidence in the reliability of the G2(+)-ECP scheme.

The coefficient of the VB triple-ion configuration $X^-R^+X^-$ in the transition state wave function can be estimated as $|Q(CH_3)|^{1/2}$, where $|Q(CH_3)|$ is the absolute magnitude of the CH_3 group charge.[4q] For X = F, this coefficient is 0.657 at the MP2 level. Using MP2 Bader charges gives a value of 0.724[4i] As the halogen electronegativity decreases, the contribution of the triple-ion configuration to the transition state wave function (given by the square of the coefficient and therefore equal to $|Q(CH_3)|$) decreases from 0.432 for X = F to just 0.098 for X = I at the MP2 level (Table 8). As mentioned above, it is possible that for X = F, it is the large contribution of the triple-ion configuration to the description of the transition state that is responsible for the relatively low energy of **2a** and a resulting negative $\Delta H^{\ddagger}_{ovr}$ value.

D. Correlations of Central Barrier Heights. 1. Correlations of Central Barriers with Reactant Properties. There has been considerable discussion in the literature as to what factors might influence barrier heights in gas-phase S_N2 reactions,[2a,23c,d,44] so we briefly consider our computational data in this context.

(40) (a) Tucker, S. C.; Truhlar, D. G. *J. Am. Chem. Soc.* **1990**, *112*, 3338. (b) Tucker, S. C.; Truhlar, D. G. *J. Phys. Chem.* **1989**, *93*, 8138.

(41) It is worth noting that reaction rates are not just governed by the height of the energy barrier, since trajectory studies suggest that barrier recrossings may occur. This means that experimental barriers that are estimated using transition state theory, which do not take barrier recrossing into account, may be somewhat overestimated. For a recent discussion of nonstatistical central barrier recrossing in the system $Cl^- + CH_3Cl$, see refs 4c,d. For a recent discussion of nonstatistical effects in non-identity S_N2 methyl-transfer reactions, see ref 3r.

(42) Keil, F.; Ahlrichs, R. *J. Am. Chem. Soc.* **1976**, *98*, 4787.

(43) Tanaka, K.; Mackay, G. I.; Payzani, J. D.; Bohme, D. K. *Can. J. Chem.* **1976**, *54*, 1643.

(44) Han, C.-C.; Dodd, J. A.; Brauman, J. I. *J. Phys. Chem.* **1986**, *90*, 471.

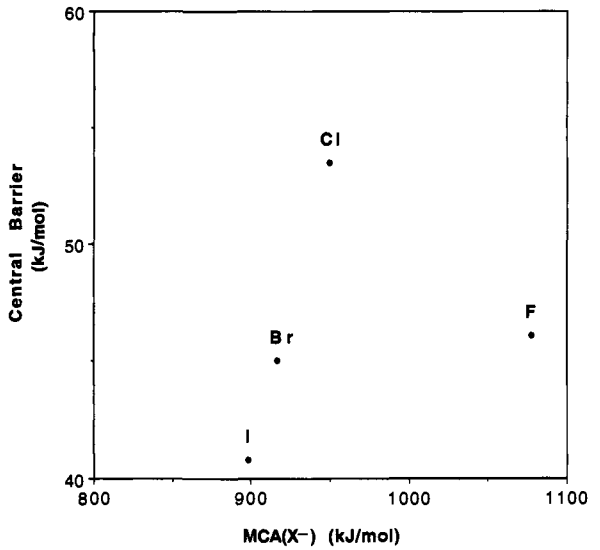

Figure 3. Plot of the G2(+) central barriers ($\Delta H^{\ddagger}_{cent}$, 298 K) for reaction 1 vs G2(+) methyl cation affinities of X^- (MCA(X^-)). The G2(+) MCA(X^-) values are given in Table 9.

Table 9. Calculated G2(+) and Experimental Methyl Cation Affinities (MCA, kJ mol^{-1}) and Proton Affinities (PA, kJ mol^{-1}) of Halide Anions (X^-) at 298 K[a]

X		G2(+) MCA[b] 0 K	G2(+) MCA[b] 298 K	exptl MCA[c] 298 K	G2(+) PA[b] 0 K	G2(+) PA[b] 298 K	exptl PA[c] 298 K
F		1070.8	1076.8	1091	1546.8	1550.5	1554 ± 1
Cl		943.3	949.0	948	1394.7	1398.4	1395 ± 1
							1396 ± 9
Br	ECP	911.2	916.7	918	1351.2	1354.9	1354
							1349 ± 9
I	ECP	893.3	898.6	890	1314.1	1317.8	1315

[a] Enthalpies of the reactions $CH_3X \rightarrow CH_3^+ + X^-$ (for MCA) and $HX \rightarrow H^+ + X^-$ (for PA). [b] For methyl cation: E(G2(+), 0 K) = −39.385 59 hartrees; E(G2(+), 298 K) = −39.381 79 hartrees. G2(+) energies of other species are given in Table 1. [c] Experimental data taken from ref 38.

A linear correlation between the experimental central barriers, $\Delta H^{\ddagger}_{cent}$, and the methyl cation affinities (MCAs) of X^- has been previously noted,[23c,d,44] although the authors indicated that it may be an artefact of the RRKM model and the Marcus analysis. Our G2 data do not show such a correlation (Figure 3; Tables 4 and 9). Similarly, we find no linear correlation between $\Delta H^{\ddagger}_{ovr}$ values and the proton affinities (PAs) of X^- (Figure 4).

According to the curve-crossing model, the barrier to an S_N2 reaction is likely to be greatly influenced by the initial energy gap between reactant and product configurations, IE(X^-) − EA(RX), where IE(X^-) and EA(RX) are gas-phase ionization energies of X^- and gas-phase vertical electron affinities of RX, respectively.[2a] This suggests that barrier heights could in some circumstances correlate with this parameter. Unfortunately, the available experimental[45] and theoretical[46] data on the vertical gas-phase electron affinity of the methyl halides vary widely, making the testing of this idea problematic. For this reason,

(45) (a) Giordan, J. C.; Moore, J. H.; Tossell, J. A. *Acc. Chem. Res.* **1986**, *19*, 281. (b) Jordan, K. D.; Burrow, P. D. *Chem. Rev.* **1987**, *87*, 557. (c) Benitez, A.; Moore, J. H.; Tossell, J. A. *J. Chem. Phys.* **1988**, *88*, 6691. (d) Krzysztofowicz, A. M.; Szmytkowski, C. *Chem. Phys. Lett.* **1994**, *219*, 86.

(46) Calculations of negative electron affinities are complicated by obtaining solutions which correspond to the neutral molecule plus a free electron. For details, see: (a) Guerra, *Chem. Phys. Lett.* **1990**, *167*, 315. (b) Simons, J.; Jordan, K. D. *Chem. Rev.* **1987**, *87*, 535. (c) Bertran, J.; Gallardo, I.; Moreno, M.; Savéant, J.-M. *J. Am. Chem. Soc.* **1992**, *114*, 9576. (d) Bertran, J.; Gallardo, I.; Moreno, M.; Savéant, J.-M. *J. Am. Chem. Soc.* **1992**, *114*, 9576. (e) Heinrich, N.; Koch, W.; Frenking, G. *Chem. Phys. Lett.* **1986**, *124*, 20.

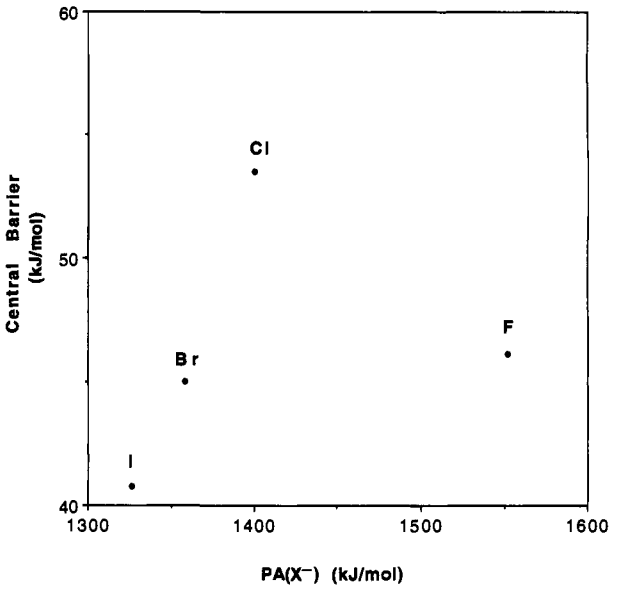

Figure 4. Plot of the G2(+) central barriers ($\Delta H^{\ddagger}_{cent}$, 298 K) for reaction 1 vs G2(+) proton affinities of X^- (PA(X^-)). The G2(+) PA(X^-) values are included in Table 9.

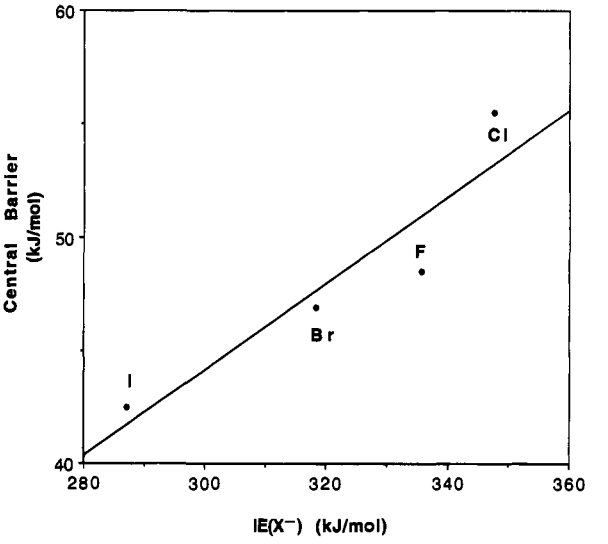

Figure 5. Plot of the G2(+) central barriers ($\Delta H^{\ddagger}_{cent}$, 0 K) for reaction 1 vs G2(+) gas-phase ionization energies of X^- (IE(X^-)). The G2(+) values of IE(X^-) (which is the same as EA(X)) are presented in Table 10.

Table 10. Calculated G2(+) and Experimental Gas-Phase Ionization Energies (IE(X^-))[a]

X =		IE(X^-) G2(+)	IE(X^-) exptl[b]
F		3.479	3.399 ± 0.003
Cl		3.602	3.617 ± 0.003
Br	ECP	3.299	3.365 ± 0.003
I	ECP	2.976	3.059

[a] All energies are given in eV. [b] Experimental data taken from ref 38.

we have not attempted to check for such a correlation. However, it is intriguing that a reasonable linear correlation is obtained between the activation barriers and IE(X^-) values (R^2 = 0.857) (Figure 5, Table 10). It is not clear whether or not this correlation is a manifestation of the implied correlation with IE(X^-) − EA(RX).

It is of interest to examine whether there is a correlation between the central S_N2 barriers, $\Delta H^{\ddagger}_{cent}$, and the D_{C-X} bond

Table 11. Calculated G2(+) and Experimental Dissociation Energies (D_{C-X}, 0 K) of the C−X Bond in CH_3X (X = F-I) and G2(+) Values of the Binding Energies of the Transition Structures **2** (E_b(TS), 0 K) and the Thermochemical Looseness Index ($T^{\ddagger}$)[a]

X =		D_{C-X} G2(+)[b]	D_{C-X} exptl[c]	E_b(TS)[d] G2(+)	$T^{\ddagger}$ [e] G2(+)
F		463.0	465.4	471.0	1.02
Cl		347.3	342.0	335.7	0.97
Br	ECP	285.9	289.9	280.2	0.98
I	ECP	237.0	231.2	230.5	0.97

[a] All energies are given in kJ mol^{-1}. The $T^{\ddagger}$ values are dimensionless. [b] The G2(+) energy of $CH_3^{\bullet}$ at 0 K is −39.744 95 hartrees. The G2(+)−ECP energies of Br(^{2}P) and I(^{2}P) (−13.108 07 and −11.337 60 hartrees) were calculated with incorporation of spin−orbit corrections; see ref 17. [c] Calculated with the use of experimental $\Delta H_{f,0}$ data taken from ref 38. $\Delta H_{f,0}$ for CH_3F was calculated from the experimental $\Delta H_{f,298}$ using theoretical enthalpy temperature corrections (see ref 12m). [d] Defined by eq 4. [e] Defined by eq 3.

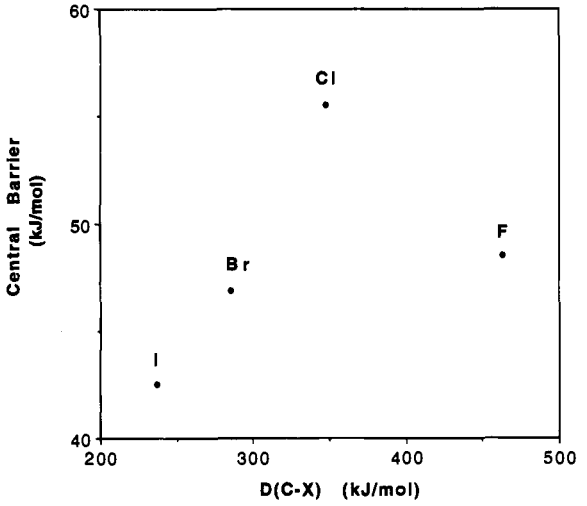

Figure 6. Plot of the G2(+) central barriers ($\Delta H^{\ddagger}_{cent}$, 0 K) for reaction 1 vs G2(+) dissociation energies of the C−X bond in CH_3X (D_{C-X}). D_{C-X} values (G2(+) and experimental, 0 K) are listed in Table 11.

dissociation energies in CH_3X (listed in Table 11). Inspection of Figure 6 indicates no such correlation. As discussed above, the similarity of the barrier heights for the different halogens, coupled with the observation that barrier heights do not correlate with either methyl cation affinity or the D_{C-X} bond dissociation energies, suggests that the bond strength factor (homolytic or heterolytic) largely cancels out due to the concurrent bond making *and* bond breaking that takes place in the transition state.

2. Correlations of Central Barriers with Energetic and Geometrical Characteristics of the Transition Structures. It has been found previously[2a,47-49] that the looseness of S_N2 transition structures with various nucleophiles, including the halide anions, X = F to I,[48] correlates with the magnitude of the activation barrier. However, for halogens, this correlation was found[47,48] with MNDO data[8] which are of questionable reliability.[5] Also, the earlier correlations for non-halogens were obtained with Hartree−Fock (HF) data,[2a,49] a level of theory that is clearly unsatisfactory since it predicts a higher barrier for X = F than that for X = Cl.

We find that at the G2(+) level of theory, there is a reasonable correlation between central barriers and the looseness of the MP2 transition structure geometries (Figure 7; $R^2 = 0.939$). This

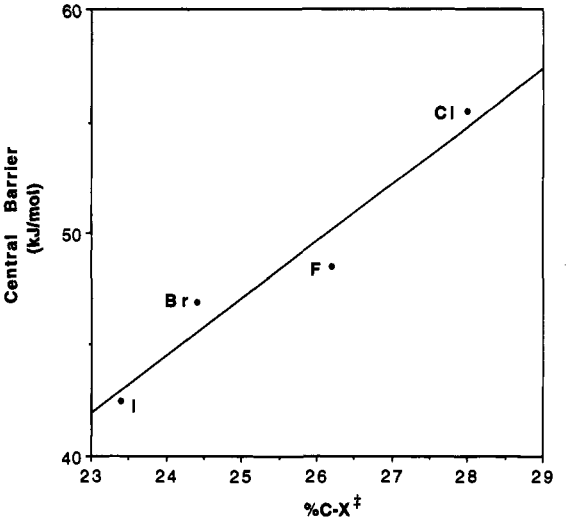

Figure 7. Plot of the G2(+) central barriers ($\Delta H^{\ddagger}_{cent}$, 0 K) for reaction 1 vs the geometric looseness index of transition structures **2** (% C−X‡) (see eq 2). The MP2/6-31+G(d) values of % C−X‡ are presented in Table 7.

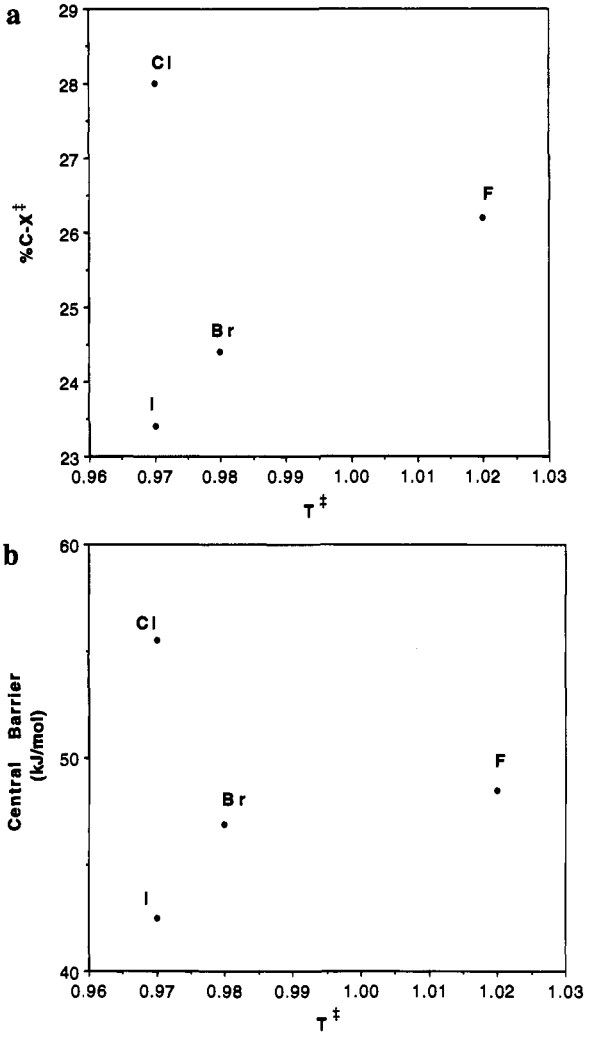

Figure 8. Plot of (a) the geometric looseness index (% C−X‡) and (b) the G2(+) central barriers ($\Delta H^{\ddagger}_{cent}$, 0 K) for reaction 1 vs the thermochemical looseness index ($T^{\ddagger}$, see eq 3). The G2(+) values of $T^{\ddagger}$ are presented in Table 11.

is true despite the inversion in the G2(+) barriers for X = F and Cl. The observed correlation reinforces the curve-crossing view that barrier formation in a chemical reaction stems from

(47) Shaik, S. S. *Acta Chem. Scand.* **1990**, *44*, 205.
(48) (a) Shaik, S. S. *Isr. J. Chem.* **1985**, *26*, 367. (b) Shaik, S. S. *Can. J. Chem.* **1986**, *64*, 96.
(49) Shaik, S. S.; Schlegel, H. B.; Wolfe, S. *J. Chem. Soc., Chem. Commun.* **1988**, 1322.

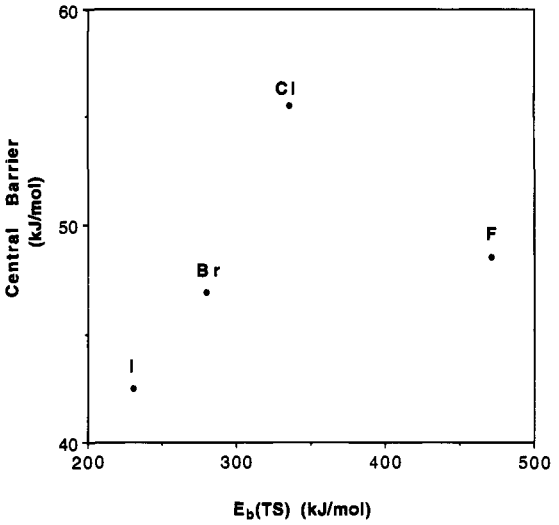

Figure 9. Plot of the G2(+) central barriers ($\Delta H^{\ddagger}_{cent}$, 0 K) for reaction 1 vs G2(+) binding energies of the transition structures (E_b(TS), 0 K) (see eq 4). The G2(+) values of E_b(TS) are presented in Table 11.

the distortions that are required to raise the energy of the reactant state in order to facilitate a crossover into the product state.[2a]

Thermochemical looseness may be expressed[50] through a thermochemical looseness index, $T^{\ddagger}$:

$$T^{\ddagger} = E_b(\text{TS})/D_{C-X} \quad (3)$$

where E_b(TS) is the binding energy of the transition structure and D_{C-X} is the C−X bond dissociation energy in CH_3X. The binding energy of the transition structure, E_b(TS), is defined by[2a]

$$E_b(\text{TS}) = E[XCH_3X^-]^{\ddagger} - E(X^{\bullet}) - E(CH_3^{\bullet}) - E(X^-) \quad (4)$$

Shaik[50] has found a correlation between the thermochemical index, $T^{\ddagger}$, and the geometric index, % C−X‡, from HF computational data for the identity S_N2 reaction. We have tested this correlation at the G2(+) level and find no correlation between $T^{\ddagger}$ and % C−X‡ (Figure 8a), or between the $T^{\ddagger}$ index and the central barriers, $\Delta H^{\ddagger}_{cent}$ (Figure 8b). It is intriguing that $\Delta H^{\ddagger}_{cent}$ correlates with % C−X‡ (Figure 7), a geometric parameter, but not with $T^{\ddagger}$ or E_b(TS) (Figure 9), both thermodynamic parameters.

(50) Shaik, S. S. *J. Am. Chem. Soc.* **1988**, *110*, 1127.

Conclusions

Application of G2(+) theory to the identity S_N2 reactions of halide anions with methyl halides (X = F, Cl, Br, and I) leads to the following conclusions.

(1) Central barrier heights ($\Delta H^{\ddagger}_{cent}$) at 298 K for X = F to I are surprisingly similar in magnitude, spanning a range of just 12.7 kJ mol^{-1}. The barrier heights decrease in the order Cl (53.5 kJ mol^{-1}) > F (46.1 kJ mol^{-1}) ≥ Br (45.0 kJ mol^{-1}) > I (40.8 kJ mol^{-1}). The high level of electron correlation and large basis sets employed in G2(+) theory are found to be essential in obtaining reliable barrier heights. The similarity in the central barrier heights despite large differences in C−X bond strengths and methyl cation affinities of the halide ions may be attributed to the fact that the transition structures for these reactions involve simultaneous bond making and bond breaking.

(2) Previously reported linear correlations of the central barrier ($\Delta H^{\ddagger}_{cent}$) with the methyl cation affinities of X$^-$ (MCA(X$^-$)), proton affinities of X$^-$ (PA(X$^-$)), and the binding energies of the transition structures, E_b(TS), are not observed at the G2(+) level. However, a reasonable correlation between $\Delta H^{\ddagger}_{cent}$ and IE(X$^-$) values is found although the significance of this correlation is not clear.

(3) Complexation energies (ΔH_{comp}) of the ion−molecule complexes X$^-\cdots$CH$_3$X (**1**) at 298 K for X = F to I decrease in the order F (57.1 kJ mol^{-1}) > Cl (43.7 kJ mol^{-1}) > Br (40.5 kJ mol^{-1}) > I (35.3 kJ mol^{-1}) and are in good agreement with experimental and earlier computational studies. Complexation energies are found to exhibit a good linear correlation with halogen electronegativity.

(4) G2(+) central barriers, $\Delta H^{\ddagger}_{cent}$, exhibit a good linear correlation with geometrical looseness (% C−X‡) of the transition structures but not with the thermochemical looseness parameter ($T^{\ddagger}$).

Acknowledgment. We gratefully acknowledge a generous allocation of time on the Fujitsu VP-2200 computer of the Australian National University Supercomputer Facility, the support of the Australian Research Council, and the award (to A.P.) of an ARC Senior Research Fellowship.

JA942587L